The 4th International Symposium - Supercritical CO2 Power Cycles
September 9-10, 2014, Pittsburgh, Pennsylvania

COMPATIBILITY OF CANDIDATE STRUCTURAL MATERIALS IN HIGH-TEMPERATURE S-CO_2 ENVIRONMENT

Ho Jung Lee
Ph.D candidate student
Korea Advanced Institute of Science and Technology
Daejeon, Rep. of Korea
leehojung@kaist.ac.kr

Hyunmyung Kim
Master degree candidate student
Korea Advanced Institute of Science and Technology
Daejeon, Rep. of Korea
h46kim@kaist.ac.kr

Changheui Jang[*]
Professor
Korea Advanced Institute of Science and Technology
Daejeon, Rep. of Korea
chjang@kaist.ac.kr

Ho Jung Lee

Bachelor degree of the Metallurgical Engineering, Yonsei university (2003-2010)

Master degree of Nuclear Materials at the Dept. of Nuclear and Quantum Engineering, Korea Advanced Institute of Science and Technology (2010-2012)

Ph.D candidate student at the Dept. of Nuclear and Quantum Engineering, Korea Advanced Institute of Science and Technology (2012-)

Hyunmyung Kim

Bachelor degree of the Nuclear and Quantum Engineering, Korea Advanced Institute of Science and Technology (2011-2013)

Master degree candidate student at the Dept. of Nuclear and Quantum Engineering, Korea Advanced Institute of Science and Technology (2013-)

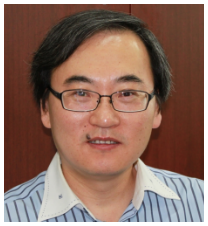

Changheui Jang[*]

Bachelor degree of Nuclear Engineering, Seoul national university, (1982-1986)

Master degree of Nuclear Materials at Dept. of Nuclear Engineering, Korea Advanced Institute of Science and Technology (1986-1988)

Ph.D of Nuclear materials at the Dept. of Nuclear Engineering, MIT (1990-1995)

Professor at the Dept. of Nuclear and Quantum Engineering, Korea Advanced Institute of Science and Technology (2004-)

ABSTRACT

For the application of super-critical CO_2 (S-CO_2) cycle for energy conversion system of Generation-IV type reactors, the compatibility and long-term integrity of candidate structural materials should be well characterized. In this study, candidate materials for heat exchangers were exposed to S-CO_2 at 550, 600, and 650 ^{o}C (200 bar) up to 1000 h, and the corrosion resistance and changes in tensile property were evaluated. The weight gains of FMS after exposure to S-CO_2 were much larger than those of Fe-base austenitic steels and Ni-base alloys in all test conditions. After exposure to S-CO_2 at the temperature ranges of 550-650 ^{o}C, tensile properties of Alloy 800 HT and Alloy 625 showed hardening and loss of ductility. Meanwhile, for SS 310S, SS 347H, Alloy 600, and Alloy 690, tensile property change was relatively small.

1. INTRODUCTION

A super-critical CO_2 (S-CO_2) Brayton cycle has been considered as one of the promising energy conversion systems in the intermediate heat exchanger (IHX) of sodium-cooled fast reactor (SFR) which could replace the steam Rankine cycle [1]. Meanwhile, from the material point of view, a compatibility of candidate materials in SFR S-CO_2 should be evaluated to assure the long-term integrity of IHX. Corrosion characteristics are one of the important factors because the poor corrosion resistance might deteriorate the heat transfer capability resulting in a negative impact on thermal efficiency. Corrosion behaviors of several types of austenitic stainless steels, Ni-base alloys, and ferritic-martensitic steels (FMS) have been investigated for SFR S-CO_2 application since the late 2000s. However, most of previous studies focused on the accelerating corrosion behaviors by increasing testing temperature to 600-650 ^{o}C [2,3] from 500-550 ^{o}C (anticipated SFR operating temperature range) to assess the long-term behaviors in short period of time [4-6]. However, there is a possibility that the mechanisms of corrosion and materials degradation may be altered by raising the test temperature too much from the operating condition. In addition to the corrosion property, long-term stabilities of the materials have to be evaluated for the selection of proper materials in SFR S-CO_2. Carburization of FMS and SS 316 was observed after long-term exposure in S-CO_2 of 550 and 650 ^{o}C at the interface between oxide and matrix depending on materials and exposure temperatures [5]. Because carburization in the matrix could accelerate degradation of mechanical properties, the effect of high temperature S-CO_2 exposure on changes in mechanical property should be evaluated.

Therefore, in this study, corrosion resistance and long-term stability of candidate structural materials were investigated at the temperatures of 550, 600, and 650 ^{o}C for 1000 h in SFR S-CO_2 environment. The corrosion resistance of candidate materials was investigated according to the type of matrix elements (Fe or Ni) with different Cr contents (9-28 wt.% Cr) as well as test temperatures. Degradation of mechanical property (changes in tensile property at room temperature) was evaluated.

2. MATERIALS AND EXPERIMENTAL

2.1 Test materials

Candidate materials for IHX used in this study are listed in Table 1. They can be divided into several types of alloys such as austenitic Fe-base steels containing around 10-30 wt.% Ni (SS 310S, SS 316H, 316LN, SS 347H, and Alloy 800HT), Ni-base alloys (Alloy 600, Alloy 625, and Alloy 690), and ferritic-martensitic steel (FMS) of G91. The selection of the candidate materials are based on 1) anticipated structural materials for SFR (SS 316H, SS316LN, and G91), 2) HX materials in the PWR reactors (Alloy 600 and Alloy 690), and 3) structural materials in advanced high temperature fossil power plants (SS 310S, SS 347H, Alloy 800HT and Alloy 625). These materials are generally known to have a high strength at the expected SFR S-CO_2 operating temperature range of 500-550 ^{o}C.

Table 1. Chemical compositions of candidate structural materials (in wt.%)

	Fe	Cr	Ni	C	Ti	Mo	Mn	Al	Si	Cu	Others
SS 310S	Bal.	24.7	19.1	.06	-	-	.8	-	.6	-	-
SS 316H	Bal.	17.3	10.7	.05	-	2.1	.6	-	.6	.2	Co : .2
SS 316LN	Bal.	18.9	13.9	.03	-	2.7	1.9	-	.6	-	N : .2
SS 347H	Bal.	18.3	8.6	.07	-	-	1.2	-	.6	-	Nb : .4
Alloy 800HT	Bal.	21.0	33.6	.06	.55	0.2	.9	.48	.4	.1	B : .003, Co : .05
Alloy 600	9.3	16.1	Bal.	.08	.20	-	.3	.16	.3	.02	B : .002
Alloy 625	4.6	22.6	Bal.	.02	.35	9.8	.04	.3	-	-	Nb : 3.1, Ta : .15
Alloy 690	8.3	28.4	Bal.	.02	.26	-	.2	.3	.2	.01	B : .002, Nb < .01
G91	Bal.	9.3	0.1	.085	-	0.9	.3	.03	.3		V: 0.19, Nb : .08

2.2 S-CO_2 corrosion test facility

Figure 1 shows the S-CO_2 corrosion test facility. The facility consists of two autoclave systems (Alloy 625) which can be operated separately at the same time. Before heating up the furnace, the system is purged with CO_2 until the amount of impurities reduced to a certain level (<1.0 ppm of O_2 and H_2O) similar to as-received high purity CO_2 (99.999 %) condition. During the test, liquid phase of CO_2 from siphon typed cylinder is supplied to a high pressure CO_2 pump at the pressure of 50 bar and pressurized at the constant flow of 3 ml/min. The temperature of S-CO_2 in the uniform region of autoclave is controlled by three zone main heaters with the range of ±2 ^{o}C. The impurity levels in the test gas are measured at the outlet of the test system using a gas analyzer and a dew point transmitter.

2.3 Corrosion and long-term integrity test

For the high temperature S-CO_2 corrosion test, materials are cut to coupon type specimens (12 mm in diameter and 1 mm in thickness) as shown in Figure 2(a). The samples are ground to 1200 grit silicon carbide grinding paper, and ultra-sonically cleaned in ethanol before the corrosion test. The isothermal corrosion tests are performed at 550, 600 and 650 ^{o}C in S-CO_2 environment of 200 bar for 1000 h as mentioned in section 2.2. The weight change is measured for two specimens of each material using a microbalance with a resolution of 0.001 mg. Then one of the samples is selected for the subsequent analyses using scanning electron microscope (SEM), and transmission electron microscope (TEM) equipped with energy dispersive spectroscopy (EDS) used to characterize the oxide layer.

For the long-term stability evaluations (changes in tensile property after long-term S-CO_2 exposure), mini-sized tensile specimens with 16 mm in length and 0.5 mm in thickness (Figure 2(b)) are also aged during the corrosion test. The tensile tests of three samples of each material are conducted at room temperature with the strain rate of 3.33×10^{-4} /s following the procedures of ASTM E8/E8M-13a. For both test specimens, a hole is drilled at the upper part of the specimen to hang it using a Pt wire while alumina spacers were placed between the test specimens on an alumina boat to prevent direct contact between the specimens as shown in Figure 2(c).

Figure 1. Corrosion test facility in S-CO_2 environment

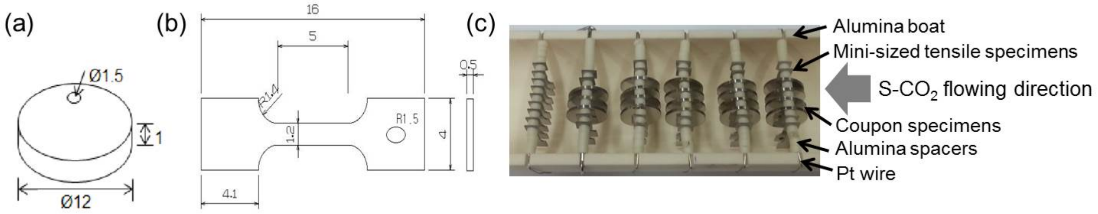

Figure 2. Geometry and dimensions of (a) coupon and (b) mini-sized tensile specimen (in mm) and the photograph of installed specimens on alumina boat

3. RESULT AND DISCUSSION

3.1 Corrosion resistance

Figure 3 shows the result of the weight gains after S-CO_2 corrosion test at 550, 600 and 650 ^oC (200 bar) for 1000 h. It indicates a tendency to increase of the weight gains as testing temperature increase from 550 to 650 ^oC. Based on the results of weight gain, three types of corrosion behaviors are recognized. First, in the case of Fe-base austenitic steels (10-30 Ni and 18-26 Cr in wt.%), SS 316H and SS 316LN exhibit significant weight gains at high temperatures. The weight gain of SS 316H increased significantly at 650 ^oC as compared to 550 and 600 ^oC while SS 316LN starts to soar at 600 ^oC. Meanwhile, the weight gains are relatively small for the other Fe-base austenitic stainless steels such as SS 310S, SS 347H, and Alloy 800HT. Overall, below 600 ^oC, corrosion resistance of Fe-base austenitic steels except SS 316LN is somewhat comparable to that of Ni-base alloys and considered rather acceptable.

On the other hand, for the Ni-base alloys (18-26 wt.% Cr) such as Alloy 600, Alloy 625, and Alloy 690, the corrosion resistance is better. However, G91 (9 wt.% Cr FMS) has a poor corrosion resistance showing the largest weigh gains compared at all test temperatures.

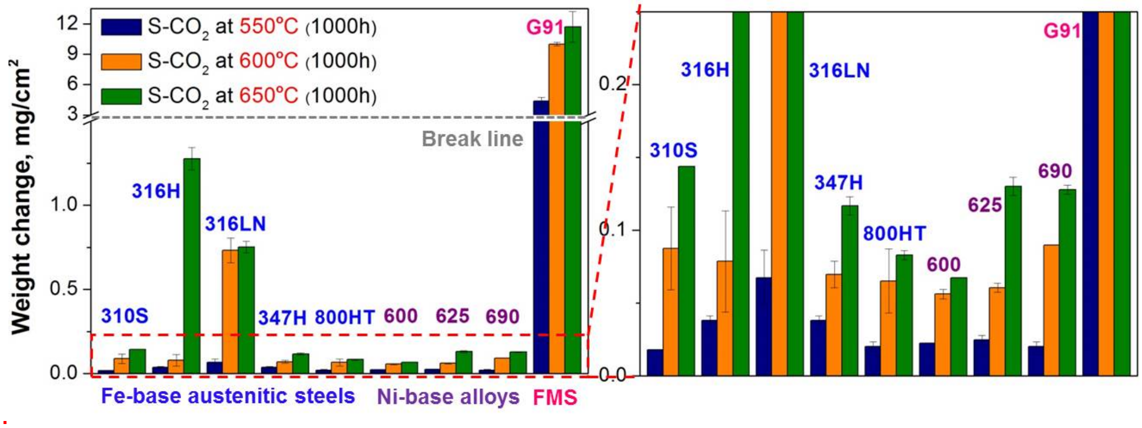

Figure 3. Results of weight gain after exposure in S-CO_2 at 550, 600 and 650 ^oC (200 bar) for 1000 h

3.2 Oxide structure

Figures 4 shows the surface oxide morphologies of SS 316H and SS 316LN (18 wt.% Cr) corroded in S-CO_2 (200 bar) at the temperature ranges of 550-650 ^oC for 1000 h. The surface oxides consist of irregular shaped Fe oxides and relatively uniform Cr-rich oxide. Fe oxide primarily has a polygonal shape, which become is much denser and larger at a higher temperature of 650 ^oC. Cr-rich oxide is a nodular (550 and 600 ^oC) or a platelet (650 ^oC) shaped. The formation of irregular Fe oxide increased at higher temperatures and covers most of the surface area at 650 ^oC for SS316H and at 600 ^oC for SS 316LN. For both materials, spallation of oxide is observed in Cr-rich oxide area at 650 ^oC. STEM analysis showed that inner Cr–rich oxide is around 200 nm thick while an outer oxide is a few μm thick for those materials. It seems that the thick outer oxide in 316H and 316LN contributed to a significant increase in weight gains at high temperatures. Therefore, the accelerated test condition of 600 ^{o}C for SS 316LN and 650 ^{o}C for 316H is too high to assess corrosion behaviors in S-CO_2 environment for the SFR application (around 500 - 550 ^{o}C) because of the strong temperature dependency of the oxidation.

On the other hand, SS 310S (25 wt.% Cr), Alloy 800 HT (21 Cr and 33 Ni in wt.%) and Ni-base alloys show different surface oxide morphologies compared to SS 316H and SS 316LN. Those alloys have similar oxide structures regardless of the temperature in the ranges of 550-650 ^{o}C as shown in Figure 5. Although isolated Fe oxides are developed on SS 310S, the size and quantity are much smaller compared to SS 316H and SS 316LN (Figure 5(a)). In addition, Fe oxides show less clear polygonal shape compared to SS 316H and SS 316LN while Cr-rich oxide has nodular (550 and 600 ^{o}C) or platelet (650 ^{o}C) shapes which are similar to SS 316H and 316LN.

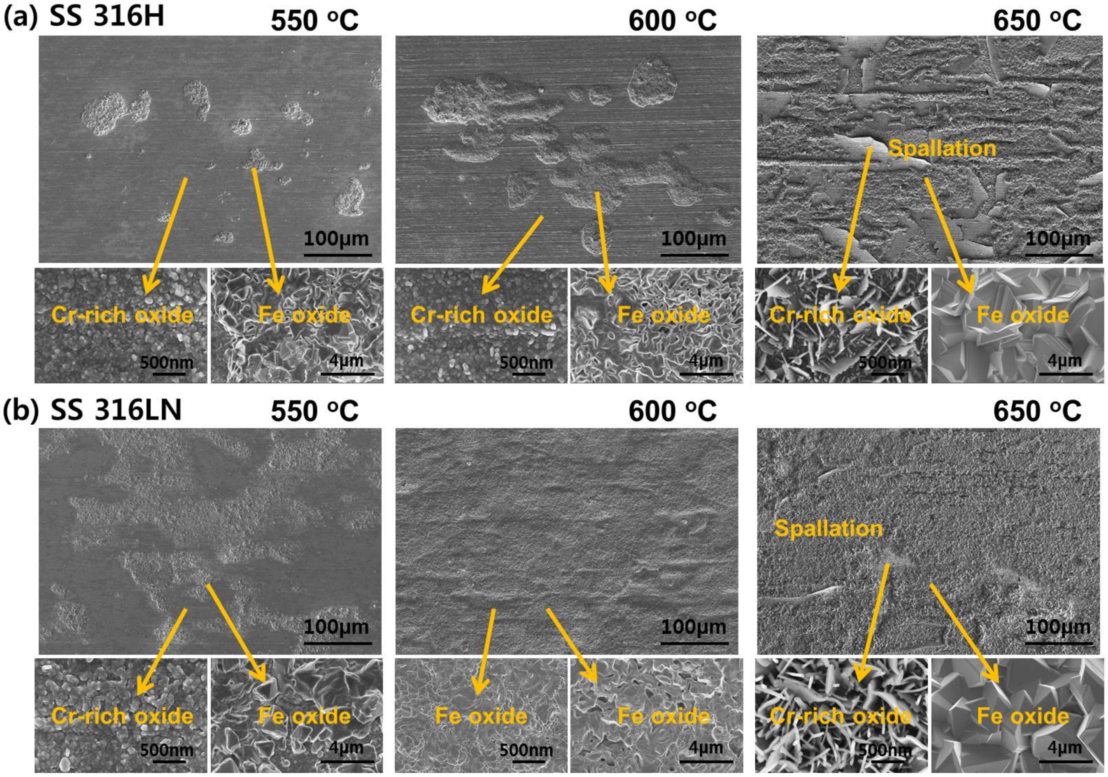

Figure 4. SEM micrographs of surface oxide morphologies of SS 316H and SS 316 LN after exposure in S-CO_2 at 550, 600 and 650 ^{o}C (200 bar) for 1000 h

For Ni-base alloys, the oxide structure is similar to SS 310S, such that the formation of Cr-rich oxide is mainly observed without Fe or Ni oxide as shown in Figure 5(b). Although Ni-spinel oxides are observed in 800HT and Alloy 625 as reported previously [6], the amount is very small compared to Cr-rich oxide. The cross-sectional STEM and EDS mapping shows that, in Alloy 600 exposed to S-CO_2 at 600 ^{o}C, Cr-rich oxide of 200 nm in thickness is developed as a major external oxide while Al and Ti-rich internal oxide is observed. Overall, in S-CO_2 environment, Ni-base alloys show a better corrosion resistance than Fe-base alloys by forming a protective Cr-rich oxide rather an outer thick Ni oxide like Fe oxide.

For G91 (9 wt.% Cr FMS), the weight gain is exceptionally large compared to Fe-base austenitic steels and Ni-base alloys (Figure 2). A polygonal shaped Fe oxide covers the outer layer uniformly at all temperatures. Different from the mixture of Fe oxide and Cr-rich oxide in Fe-base austenitic steels (18-26 wt.% Cr), a relatively low Cr content in FMS seems not enough to form protective Cr-rich oxide and resulted in the worst corrosion resistance among the test materials.

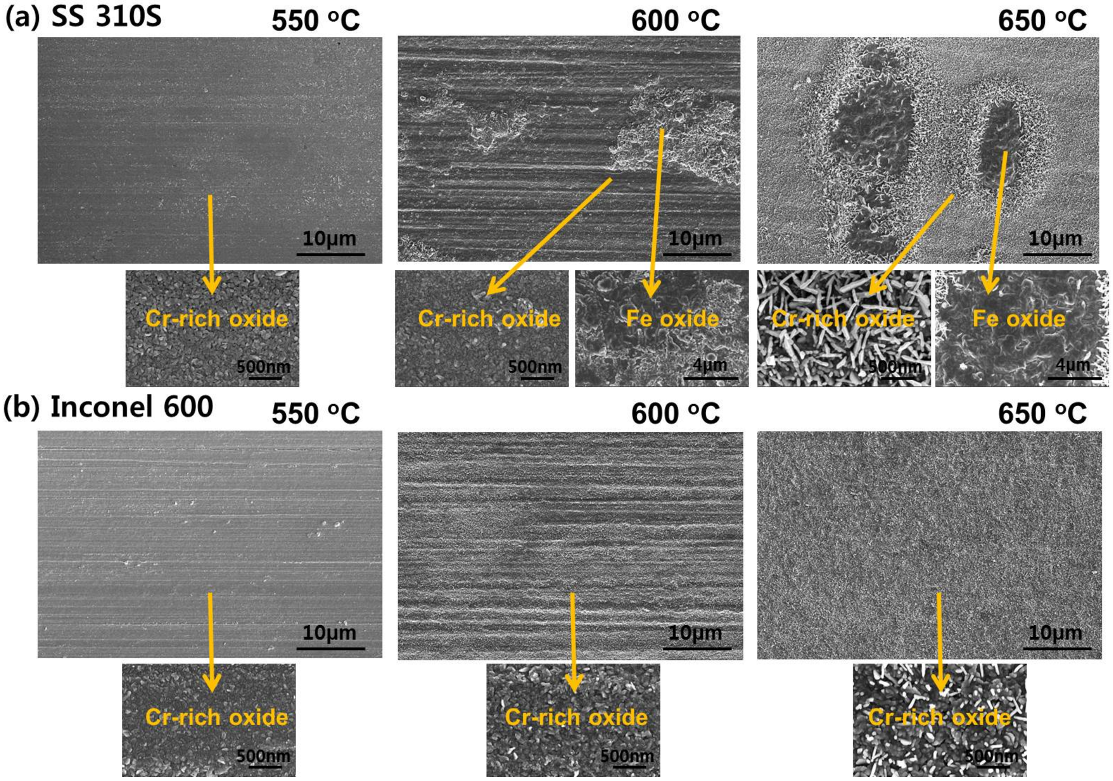

Figure 5. SEM micrographs of surface oxide morphologies of SS 310S and Inconel 600 after exposure in $S\text{-}CO_2$ at 550, 600 and 650 °C (200 bar) for 1000 h

3.3 Changes in tensile property after exposure in $S\text{-}CO_2$

Figure 6 represents preliminary results of room temperature tensile properties of mini-sized specimens after aging in $S\text{-}CO_2$ at 550, 600 and 650 °C for 1000 h. Further test up to 3,000 h are in progress. As shown in the figure, ultimate tensile strength (UTS) of Alloy 800 HT and Alloy 625 increased significantly as the exposure temperature increased from 550 to 650 °C along with significant reduction in ductility. The significant increase in strength could have been caused by the precipitation of secondary phases containing Al, Ti and Nb. In this case accelerated test at higher temperature may not be appropriate for these materials. Meanwhile, in case of SS 310S, SS 347H, Alloy 600, and Alloy 690, changes in tensile properties such as UTS and elongation are rather small in all test conditions. For G91, UTS increases up to 600 °C exposure but decrease after exposure at 650 °C, while elongation decreases steadily up to 650 °C. Further microstructural analyses are being conducted to understand the corrosion resistance and the effects of aging in $S\text{-}CO_2$ environments. Also, the possible interaction between the corrosion resistance and mechanical behaviors of the candidate materials in SFR S-CO_2 environments is investigated. The results of the analysis will be presented at the conference.

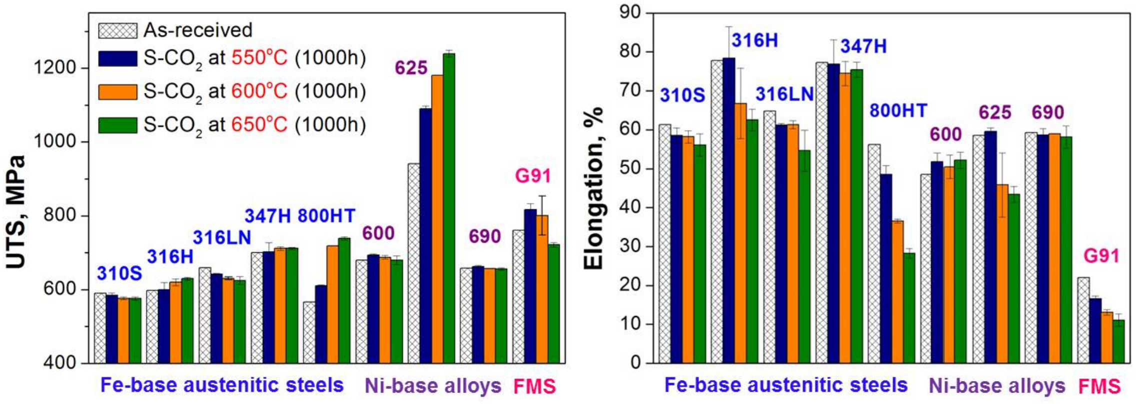

Figure 6. The changes in tensile properties at room temperature after exposure in S-CO_2 at 550, 600 and 650 ^oC (200 bar) for 1000 h

4. CONCLUSION

Isothermal corrosion tests and aging of candidate materials for IHX in SFR S-CO_2 system were carried out in S-CO_2 environment (200 bar) at 550, 600, and 650 ^oC up to 1000 h. Based on the tests and subsequent analyses, the following conclusions were drawn;

1. The weight gains of FMS are significantly larger than those of Fe-base austenitic steels and Ni-base alloys in all test conditions. At 550 ^oC, both Fe-base austenitic steels and Ni-base alloys show a good corrosion resistance which could be applicable to SFR S-CO_2 environment.
2. In the case of Fe-base austenitic steels, the surface oxides consist of the mixture of polygonal shaped Fe oxide and nodular (550 and 600 ^oC) or platelet (650 ^oC) shaped Cr-rich oxide. For SS 316H and SS 316LN, the corrosion resistance is strongly dependent on test temperatures resulted from the formation of thick outer Fe oxide.
3. The room temperature tensile properties of for Alloy 800 HT and Alloy 625 showed large hardening and loss of ductility after exposure to S-CO_2 at the temperature ranges of 550-650 ^oC. Meanwhile, in case of SS 310S, SS 347H, Alloy 600, and Alloy 690, changes in tensile properties such as UTS and elongation are rather small in all test conditions.

ACKNOWLEDGEMENTS

This study was supported by the MSIP/NRF (Nuclear R&D Program 2013M2A8A6035683) of Korea. One of the authors is also supported by the Global Ph. D Fellowship Program supported by MSIP /NRF of Korea

REFERENCES

1. Chang, Y.I., Finck , P.J., Grandy, C., 2006, “Advanced Burner Test Reactor Preconceptual Design Report”, Argonne National Laboratory report ANL-ABR-1 (ANL-AFCI-173).

2. Cao, G., Firouzdor, V., Sridharan, K., Anderson, M., Allen, T.R., 2012, “Corrosion of Austenitic Alloys in High Temperature Supercritical Carbon Dioxide”, Corrosion Science, 60, 246-255.

3. Sridharan, K., Anderson, M., Cao, G., Jelinek, J., Firouzdor, V., Allen, T.R., 2011, “Corrosion Testing of Materials in High Temperature Supercritical Carbon-dioxide Environment”, Supercritical CO_2 Power Cycle Symposium, May 24-25, Boulder, Colorado.

4. Rouillard, F., Charton, F., Moine, G., 2009, “Corrosion Behavior of Different Metallic Materials in Supercritical CO_2 at 550 ^oC and 250 bar”, Supercritical CO_2 Power Cycle Symposium, April 29-30, Troy, NY.

5. Furukawa, T., Inagaki, Y., Aritomi, M., 2011, “Compatibility of FBR Structural Materials with Supercritical Carbon Dioxide”, Progress in Nuclear Energy, 53, 1050-1055.

6. Anderson, M., 2012, “Materials, Turbomachinery and Heat Exchangers for Supercritical CO_2 Systems”, Project Report of Nuclear Energy University Program 09-778, University of Wisconsin.